Emergence of quasi-condensates of hard-core bosons at finite momentum

Marcos Rigol and Alejandro Muramatsu
Institut für Theoretische Physik III, Universität Stuttgart,
Pfaffenwaldring 57, D-70550 Stuttgart, Germany.

An exact treatment of the non-equilibrium dynamics of hard-core bosons on one-dimensional lattices shows that, starting from a pure Fock state, quasi-long-range correlations develop dynamically, and that they lead to the formation of quasi-condensates at finite momenta. Scaling relations characterizing the quasi-condensate and the dynamics of its formation are obtained. The relevance of our findings for atom lasers with full control of the wave-length by means of a lattice is discussed.

PACS numbers: 03.75.Kk, 03.75.Lm, 03.75.Pp, 05.30.Jp

The study of the non-equilibrium dynamics of quantum gases has been shown to be a very useful tool for the understanding of their properties [1]. Since the achievement of Bose-Einstein condensation (BEC) [2], where the anisotropic expansion of the gas revealed the importance of the inter-particle interaction, many experiments studying the dynamics of such systems have been developed. Recently, the possibility of realizing one-dimensional (1-D) quantum gases has attracted a lot of attention. They can be obtained experimentally in very elongated traps [3], or using optical lattices [4]. In these quasi-1D systems it is possible to go from the weakly interacting regime to an impenetrable gas of bosons, i.e. hard-core bosons (HCB) [5]. Theoretical studies have analyzed the density evolution between these two extreme regimes [6], showing that in general it does not follow a self-similar solution. In addition, in the HCB limit the Fermi-Bose mapping [7] was generalized to the time-dependent case, where the density dynamics revealed dark soliton structures, breakdown of the time-dependent mean-field theory, and interference patterns of the thermal gas on a ring [8].

In 1D systems in equilibrium it was shown that quasi-condensates of HCB develop in the homogeneous [9], harmonically trapped [10], and in general cases in the presence of a lattice [11]. This is because the ground state of these systems exhibits off-diagonal quasi-long-range order determined by a power-law decay of the one-particle density matrix (OPDM) $\rho_{ij} \sim |x_i - x_j|^{-1/2}$ [9, 11], i.e. there is no BEC in the thermodynamic limit [12]. The occupation of the lowest natural orbital (NO) (the highest occupied one) is then proportional to $\sqrt{N_b}$ (N_b being the number of HCB) [9, 10, 11]. The NO (ϕ_i^η) are effective single particle states defined as the eigenstates of the OPDM [13], i.e. they are obtained by the equation $\sum_j \rho_{ij}\phi_j^\eta = \lambda_\eta \phi_i^\eta$, with λ_η being their occupations.

In the present work we study within an *exact* approach the non-equilibrium dynamics of HCB in 1D configurations with an underlying lattice. The presence of the lattice enhances correlations between particles, and its experimental realization (the so-called optical lattice) allowed the study of the Mott superfluid-insulator transition for soft-core bosons [14]. In contrast to the continuous case, in a lattice it is possible to create pure Fock states of HCB (a HCB per lattice site) where there is no coherence in the system. We show that quasi-long-range correlations develop in the equal-time-one-particle density matrix (ETOPDM) when such states are allowed to evolve freely, and that they lead to the formation of quasi-condensates of HCB at finite momentum. In addition we obtain an universal power law describing the population of the quasi-condensate as a function of time, independent of the initial number of particles in the Fock-state. Finally, we analyze how such systems can be used to create atom lasers with a wave-length that can be controlled through the lattice parameter. Our analysis is based on a generalization of the method used to study the ground-state properties of 1D HCB on a lattice [11].

The HCB Hamiltonian on a lattice can be written as

$$H_{HCB} = -t \sum_i \left(b_i^\dagger b_{i+1} + h.c. \right) + V_\alpha \sum_i x_i^\alpha \; n_i, \qquad (1)$$

with the addition of the on-site constraints for the creation ($b_i^\dagger$) and annihilation (b_i) operators: $b_i^{\dagger 2} = b_i^2 = 0$, and $\left\{ b_i, b_i^\dagger \right\} = 1$. The hopping parameter is denoted by t and $n_i = b_i^\dagger b_i$ is the particle number operator. The last term in Eq. (1) describes an arbitrary confining potential.

The Jordan-Wigner transformation [15],

$$b_i^\dagger = f_i^\dagger \prod_{\beta=1}^{i-1} e^{-i\pi f_\beta^\dagger f_\beta}, \quad b_i = \prod_{\beta=1}^{i-1} e^{i\pi f_\beta^\dagger f_\beta} f_i \; , \qquad (2)$$

is used to map the HCB Hamiltonian into the one of non-interacting fermions

$$H_F = -t \sum_i \left(f_i^\dagger f_{i+1} + h.c. \right) + V_\alpha \sum_i x_i^\alpha \; n_i^f, \qquad (3)$$

where $f_i^\dagger$ and f_i are the creation and annihilation operators for spinless fermions, and $n_i^f = f_i^\dagger f_i$.

This mapping allows to express the equal-time Green's function for the HCB in a non-equilibrium system as

$$\begin{aligned} G_{ij}(\tau) &= \langle \Psi_{HCB}(\tau) | b_i b_j^\dagger | \Psi_{HCB}(\tau) \rangle \qquad (4) \\ &= \langle \Psi_F(\tau) | \prod_{\beta=1}^{i-1} e^{i\pi f_\beta^\dagger f_\beta} f_i f_j^\dagger \prod_{\gamma=1}^{j-1} e^{-i\pi f_\gamma^\dagger f_\gamma} | \Psi_F(\tau) \rangle, \end{aligned}$$

where τ is the real time variable, $|\Psi^G_{HCB}(\tau)\rangle$ is the time evolving wave-function for the HCB and $|\Psi^G_F(\tau)\rangle$ is the corresponding one for the non-interacting fermions.

In what follows, we study the time evolution of initial Fock states of HCB once they are allowed to evolve freely. Experimentally such states can be created by a strong confining potential $V_\alpha(N_b a/2)^\alpha \gg t$ (a is the lattice constant), which avoid vacancies. Since the equivalent fermionic system is a non-interacting one, the time evolution of an initial wave-function ($|\Psi^I_F\rangle$) can be easily calculated

$$|\Psi_F(\tau)\rangle = e^{-iH_F\tau/\hbar}|\Psi^I_F\rangle = \prod_{\delta=1}^{N_f}\sum_{\sigma=1}^{N} P_{\sigma\delta}(\tau) f^\dagger_\sigma\,|0\rangle, \quad (5)$$

which is a product of single particle states, with N_f being the number of fermions ($N_f = N_b$), N the number of lattice sites and $\mathbf{P}(\tau)$ the matrix of components of $|\Psi_F(\tau)\rangle$. From here on the method is identical to the one used in Ref. [11], the action of $\prod_{\gamma=1}^{j-1} e^{-i\pi f^\dagger_\gamma f_\gamma}$ on the right in Eq. (4) generates only a change of sign on the elements $P_{\sigma\delta}(\tau)$ for $\sigma \leq j-1$, and the further creation of a particle at site j implies the addition of one column to $\mathbf{P}(\tau)$ with the element $P_{jN_f+1}(\tau) = 1$ and all the others equal to zero (the same applies to the action of $\prod_{\beta=1}^{i-1} e^{i\pi f^\dagger_\beta f_\beta} f_i$ on the left of Eq. (4)). Then the HCB Green's function can be calculated exactly as [11]

$$\begin{aligned} G_{ij}(\tau) &= \langle 0|\prod_{\delta=1}^{N_f+1}\sum_{\beta=1}^{N} P'^A_{\beta\delta}(\tau) f_\beta \prod_{\sigma=1}^{N_f+1}\sum_{\gamma=1}^{N} P'^B_{\gamma\sigma}(\tau) f^\dagger_\gamma\,|0\rangle \\ &= \det\left[\left(\mathbf{P}'^A(\tau)\right)^\dagger \mathbf{P}'^B(\tau)\right], \end{aligned} \quad (6)$$

where $\mathbf{P}'^A(\tau)$ and $\mathbf{P}'^B(\tau)$ are the new matrices obtained from $\mathbf{P}(\tau)$ when the required signs are changed and the new columns added. The evaluation of $G_{ij}(\tau)$ is done numerically, and the ETOPDM ($\rho_{ij}(\tau)$) is determined by the expression $\rho_{ij}(\tau) = \left\langle b^\dagger_i b_j \right\rangle_\tau = G_{ji}(\tau) + \delta_{ij}\,(1 - 2G_{ii}(\tau))$.

Figure 1 shows density profiles (a), and their corresponding momentum distribution functions (MDF) (b) for the time evolution of an initial Fock state. Initially, the MDF is flat as corresponds to a pure Fock state, and during the evolution of the system sharp peaks appear at $k = \pm\pi/2a$. Notice that although in the equivalent fermionic system the density profiles are equal to the ones of the HCB, the MDF remains flat since the fermions do not interact, making evident the non-trivial differences in the off-diagonal correlations between both systems.

Since the peaks in the MDF may correspond to quasi-condensates at finite momenta, we diagonalize the ETOPDM to study the NO. In Fig. 2(a) we show the lowest NO ($|\phi^0|$ since ϕ^0 is complex) corresponding to the results in Fig. 1 for $\tau > 0$ (at $\tau = 0$ the NO are

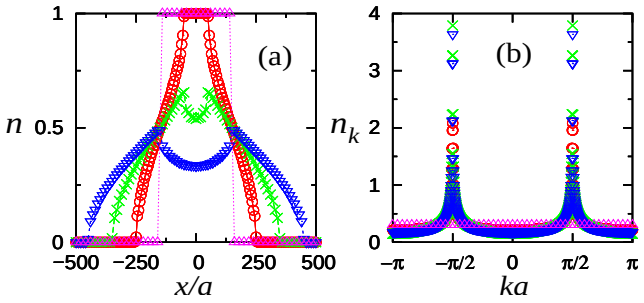

FIG. 1: (color online). Evolution of density (a) and momentum (b) profiles of 300 HCB in 1000 lattice sites. The times are $\tau = 0$ (△), $50\hbar/t$ (◯), $100\hbar/t$ (×), and $150\hbar/t$ (▽). Positions (a) and momenta (b) are normalized by the lattice constant a.

delta functions at the occupied sites). They are two-fold degenerate, corresponding to right- (for $x > 0$) and left- (for $x < 0$) moving solutions. It can be seen that some time after the $n = 1$ plateau disappears from the system, the NO lobes almost do not change their form and size (see inset in Fig. 2(a) for the right lobe at three different times). Furthermore, they move with constant velocities $v_{NO} = \pm 2at/\hbar$ (see inset in Fig. 2(b) for the positive one). These are in fact, the group velocities $v = 1/\hbar\ \partial\epsilon_k/\partial k$ for a dispersion $\epsilon_k = -2t\cos ka$ (the one of HCB on a lattice) at $k = \pm\pi/2a$. This is further confirmed by considering the Fourier transforms of the lowest NO Fig. 2(b), which show sharp peaks centered at quasi-momenta $k = \pm\pi/2a$. The peak at $k = +\pi/2a$ appears due to the Fourier transform of the right lobe in Fig. 2 (a) (i.e. $\phi^0_i \approx |\phi^0_i| e^{i\pi x_i/2a}$ for $x_i > 0$), and the one at $k = -\pi/2a$ due to the fourier transform of the left lobe (i.e. $\phi^0_i \approx |\phi^0_i| e^{-i\pi x_i/2a}$ for $x_i < 0$). Studying the Fourier transform of the other NO we have seen that they have very small or zero weight at $k = \pm\pi/2a$ so that we can conclude that the peaks at $n_{k=\pm\pi/2a}$ are reflecting the large occupation of the lowest NO.

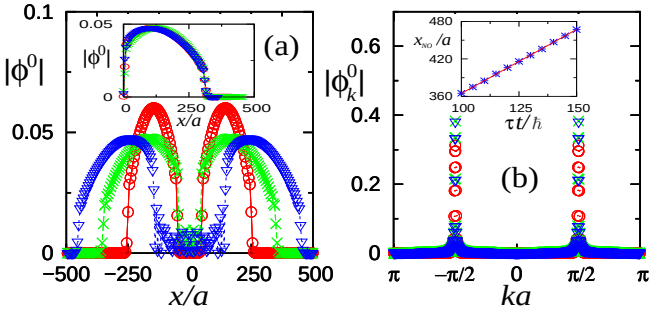

FIG. 2: (color online). Lowest NO evolution (a) and its fourier transform (b). The times are $\tau = 50\hbar/t$ (◯), $100\hbar/t$ (×), and $150\hbar/t$ (▽). The insets show: (a) the superposed right lobe of the lowest NO at $\tau = 100\hbar/t$ (×), $125\hbar/t$ (◯), and $150\hbar/t$ (▽); (b) the evolution of the lowest NO right lobe position, the line has a slope 2.

Whether the large occupation of the lowest NO corresponds to a quasi-condensate, can be determined studying the ETOPDM. Fig. 3(a) shows the results for $|\rho_{ij}|$ (with i taken at the beginning of the lowest NO left lobe's and $j > i$) at the same times of Figs. 1, 2. It can be seen that off-diagonal quasi-long-range order develops in the ETOPDM. It is reflected by a power-law decay of the form $|\rho_{ij}| = 0.25\ |(x_i - x_j)/a|^{-1/2}$, that remains almost unchanged during the evolution of the system. A careful inspection shows that this power-law behavior is restricted to the regions where each lobe of the lowest NO exists, outside these regions the ETOPDM decays faster. This quasi-coherent behavior in two different segments of the system is the reason for the degeneracy found in the lowest NO. In addition, a detailed analysis of the ETOPDM Fourier's transform shows that the peak in the MDF at $k = +\pi/2a$ is originated by components of the ETOPDM with $x_i, x_j > 0$, and the one at $k = -\pi/2a$ by the components with $x_i, x_j < 0$, so that in the regions of the lobes $\rho_{ij} \approx 0.25\ |(x_i - x_j)/a|^{-1/2} e^{i\pi(x_i - x_j)/2a}$ for $x_i, x_j > 0$, and $\rho_{ij} \approx 0.25\ |(x_i - x_j)/a|^{-1/2} e^{-i\pi(x_i - x_j)/2a}$ for $x_i, x_j < 0$. The prefactor of the power law (0.25) was found to be independent of the number of particles in the initial Fock state.

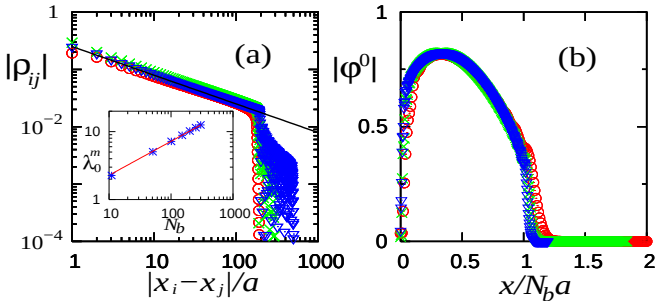

FIG. 3: (color online). (a) ETOPDM for: τ=50$\hbar/t$ (◯), 100$\hbar/t$ (×), and 150$\hbar/t$ (▽), the line is 0.25 $|(x_i - x_j)/a|^{-1/2}$ (see text for details). (b) Scaled lowest NO right lobe's *vs* $x/N_b a$ for $N_b = 101$ (◯), 201 (×), and 301 (▽). The inset in (a) shows the maximum occupation of the lowest NO *vs* N_b of the initial Fock state, the line is 0.72 $N_b^{1/2}$.

After having observed off-diagonal quasi-long-range correlations in the ETOPDM, it remains to consider how the occupation of the lowest NO behaves in the thermodynamic limit, in order to see whether it corresponds to a quasi-condensate. The only new information we need at this point is the scaling relation (if any) of the modulus of the lowest NO with the number of particles in the initial Fock state. For this, we consider the NO at those times, where as shown in the inset of Fig. 2, they almost do not change in time, i.e. after the plateau with $n = 1$ disappears. In Fig. 3(b) we show that a scaled NO ($|\varphi_0| = N_b^{1/2} |\phi^0|$) exists when its size is normalized by $N_b a$. (The results for the left lobe are identical due to inversion symmetry.) Figure 3(b) also shows that the lobe size L is approximately $N_b a$. Then evaluating $\lambda_0 = \sum_{ij} \phi_i^{*0} \rho_{ij} \phi_j^0$ as the double of the integral over a single lobe ($L \gg a$) one obtains

$$\lambda_0 \sim 2/a^2 \int_0^L dx \int_0^L dy\ \phi^{*0}(x) \rho(x,y) \phi^0(y) \qquad (7)$$
$$= N_b^{1/2} \int_0^1 dX \int_0^1 dY \frac{|\varphi^0(X)| 0.25 |\varphi^0(Y)|}{|X - Y|^{-1/2}} = A\sqrt{N_b},$$

where we did the change of variables x=$X N_b a$, y=$Y N_b a$, ϕ^0=$N_b^{-1/2} \varphi^0$, and we notice that the phase factors between the NO and the ETOPDM cancel out. The integral over X, Y is a constant that we call A. A confirmation of the validity of the previous calculation is shown in the inset of Fig. 3(a). There we plot the maximum occupation of the lowest NO (reached when the lobes of the NO have a stable form), as a function of the number of particles in the initial Fock state. The $\sqrt{N_b}$ power-law behavior is evident and a fit allowed to obtain the constant $A = 0.72$. Hence, this and the previous results demonstrate that the peaks of the MDF in Fig. 1(b) correspond to quasi-condensates with momenta $k = \pm\pi/2a$.

The appearance of such quasi-condensates at $k = \pm\pi/2a$ can be understood on the basis of total energy conservation. Given the dispersion relation of HCB on a lattice, since the initial Fock state has a flat MDF, its total energy is $E_T = 0$. Would all the particles condense into one state, it would be the one with an energy corresponding to $\overline{\epsilon}_k = E_T/N$. Taking into account the dispersion relation for HCB on a lattice ($\epsilon_k = -2t \cos ka$), $\overline{\epsilon}_k = 0$ corresponds to $k = \pm\pi/2a$. Actually, in the 1D case there is only quasi-condensation, so that the argument above applies only to maximize the occupation of a given state. In addition, the minimum in the density of states at these quasi-momenta reinforces quasi-condensation into a single momentum state.

The process of formation of the quasi-condensate is also characterized by a power law. In Fig. 4(a) we plot the occupation of the lowest NO as a function of the evolution time. The *log-log* scale shows that the occupation of the quasi-condensate increases quickly and decays slowly. A more detailed examination shows that the population of the quasi-condensate increases in an universal way ($1.38\sqrt{\tau t/\hbar}$, continuous line in Fig. 4(a)) independently of the initial number of particles in the Fock state. The power law is determined by the universal behavior of the off-diagonal part of the ETOPDM shown before, and the fact that during the formation of the quasi-condensate, the NO increases its size linearly with time at a rate given by $|v_{NO}| = 2at/\hbar$. Such a power law is followed almost up to the point where the maximal occupation is reached. The time at which it is reached depends linearly on the number of particles of the initial Fock state $\tau_m = 0.32 N_b \hbar/t$ as shown in the inset of Fig. 4(a). For a tipical experimental setup of rubidium

atoms, in a lattice with a recoil energy of $E_r = 20$kHz and a depth of $20E_r$, the time τ_m can be estimated as $\tau_m \sim 5.7N_b$(ms).

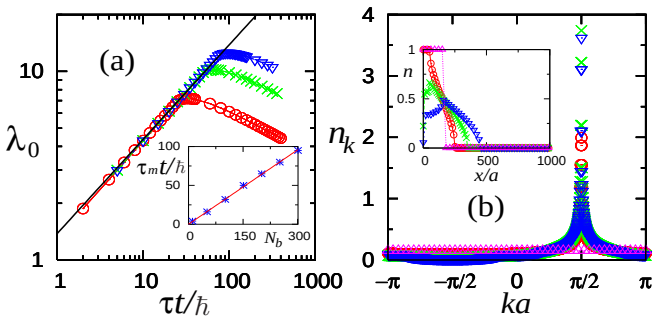

FIG. 4: (color online). (a) Time evolution of the lowest NO occupation for $N_b = 101$ (◯), 201 (×), and 301 (▽), the straight line is $1.38\sqrt{\tau t/\hbar}$. The inset shows the time at which the maximum occupation of the NO is reached ($\tau_m t/\hbar$) *vs* N_b, the line is $0.32N_b$. (b) Density profiles (inset) and MDF of 150 HCB evolving only to the right in 1000 lattice sites for $\tau = 0$ (△), $50\hbar/t$ (◯), $100\hbar/t$ (×), and $150\hbar/t$ (▽).

The results above showing that a quasi-coherent matter front forms spontaneously from Fock states of HCB, suggest that such an arrangement could be used to create atom lasers with a wave-length that can be fully controlled given the lattice parameter a. No additional effort is needed to separate the quasi-coherent part from the rest since the quasi-condensate is traveling at the maximum possible velocity on the lattice so that the front part of the expanding cloud is the quasi-coherent part. The actual realization would imply to restrict the evolution of the initial Fock state to one direction, as shown in Fig. 4(b), where we display the MDF for 150 HCB restricted to evolve to the right in 1000 lattice sites at the same evolution times of Fig. 1. It can be seen that the values of $n_{k=\pi/2}(\tau)$ are almost the same in both situations, although in Fig. 4(b) the initial Fock state has almost half of the particles. The same occurs to the occupation of the lowest NO that in the latter case is not degenerated anymore.

The previous results suggest how to proceed in order to obtain lasers in higher dimensional systems where real condensation can occur [16]. One can employ Mott insulator states with one particle per lattice site created by a very strong on-site repulsive potential U. The latter is required in order to obtain a close realization of a pure Fock state, since quantum fluctuations of the particle number present in a Mott insulator for any finite U [17] will be strongly suppressed. Then the geometry of the lattice should be designed in order to restrict the evolution of the Mott insulator to one direction only, and to have a low density of states around the mean value of energy per particle in the initial state. With these conditions the sharp features observed in 1D should be reproduced by a condensate in higher dimensions.

In summary, we have studied the non-equilibrium dynamics of a Fock states of HCB when they are allowed to evolve freely. We have shown that quasi-long-range correlations develop dynamically in these systems and that they lead to the formation of quasi-condensates of HCB at quasi-momenta $k \pm \pi/2a$. We have studied the dynamics of the formation of these quasi-condensates, and their occupations were found to scale proportionally to $\sqrt{N_b}$. These systems can be used to create atom lasers since the quasi-condensate develops quickly and decays slowly. The wave-length of such lasers is simply determined by the lattice parameter. Finally, we have discussed the possibility of creating atom lasers in higher dimensional systems where true condensation can occur.

We thank HLR-Stuttgart (Project DynMet) for allocation of computer time, and SFB 382 for financial support. We are gratefull to F. de León for useful discussions.

[1] F. Dalfovo, S. Giorgini, L. P. Pitaevskii and S. Stringari, Rev. Mod. Phys. **71**, 463 (1999).
[2] M. H. Anderson *et al.*, Science **269**, 198 (1995); C. C. Bradley *et al.*, Phys. Rev. Lett. **75**, 1687 (1995); K. B. Davis *et al.*, Phys. Rev. Lett. **75**, 3969 (1995).
[3] F. Schreck *et al.*, Phys. Rev. Lett. **87**, 080403 (2001); A. Görlitz *et al.*, Phys. Rev. Lett. **87**, 130402 (2001).
[4] M. Greiner *et al.*, Phys. Rev. Lett. **87**, 160405 (2001); H. Moritz *et al.*, Phys. Rev. Lett. **91**, 250402 (2003); T. Stöferle *et al.*, Phys. Rev. Lett. **92**, 130403 (2004).
[5] M. Olshanii, Phys. Rev. Lett. **81**, 938 (1998); D. S. Petrov, G. V. Shlyapnikov, and J. T. M. Walraven, Phys. Rev. Lett. **85**, 3745 (2000); V. Dunjko, V. Lorent, and M. Olshanii, Phys. Rev. Lett. **86**, 5413 (2001).
[6] P. Öhberg and L. Santos, Phys. Rev. Lett. **89**, 240402 (2002); P. Pedri, L. Santos, P. Öhberg, and S. Stringari, Phys. Rev. A **68**, 043601 (2003).
[7] M. Girardeau, J. Math. Phys. **1**, 516 (1960).
[8] M. D. Girardeau and E. M. Wright, Phys. Rev. Lett. **84**, 5691 (2000); M. D. Girardeau and E. M. Wright, Phys. Rev. Lett. **84**, 5239 (2000); K. K. Das, M. D. Girardeau, and E. M. Wright, Phys. Rev. Lett. **89**, 170404 (2002).
[9] A. Lenard, J. Math. Phys. **5**, 930 (1964), H. G. Vaidya and C. A. Tracy, Phys. Rev. Lett. **42**, 3 (1979).
[10] M.D. Girardeau, E.M. Wright, and J.M. Triscari, Phys. Rev. A **63**, 033601 (2001); T. Papenbrock, Phys. Rev. A **67**, 041601(R) (2003); P.J. Forrester, N.E. Frankel, T.M. Garoni, and N.S. Witte, Phys. Rev. A **67**, 043607 (2003).
[11] M. Rigol and A. Muramatsu, Phys. Rev. A **70**, 031603(R) (2004).
[12] C. N. Yang, Rev. Mod. Phys. **34**, 694 (1962).
[13] O. Penrose and L. Onsager, Phys. Rev. **104**, 576 (1956).
[14] D. Jaksch *et al.*, Phys. Rev. Lett. **81**, 3108 (1998); M. Greiner *et al.*, Nature **415**, 39 (2002).
[15] P. Jordan and E. Wigner, Z. Phys. **47**, 631 (1928).
[16] E. H. Lieb and R. Seiringer, Phys. Rev. Lett. **88**, 170409 (2002).
[17] G. G. Batrouni *et al.*, Phys. Rev. Lett. **89**, 117203 (2002); M. Rigol, A. Muramatsu, G. G. Batrouni, and R. T. Scalettar, Phys. Rev. Lett. **91**, 130403 (2003).